



Universiteit  
Leiden  
The Netherlands

## **Anyonic, cosmic, and chaotic: three faces of Majorana fermions**

Cheipesh, Y.I.

### **Citation**

Cheipesh, Y. I. (2022, November 17). *Anyonic, cosmic, and chaotic: three faces of Majorana fermions*. *Casimir PhD Series*. Retrieved from <https://hdl.handle.net/1887/3487143>

Version: Publisher's Version

License: [Licence agreement concerning inclusion of doctoral thesis in the Institutional Repository of the University of Leiden](#)

Downloaded from: <https://hdl.handle.net/1887/3487143>

**Note:** To cite this publication please use the final published version (if applicable).

# Chapter 8

## Screening effects in the graphene-based relic neutrino detection experiment

### 8.1 Introduction.

The detection of the Cosmic Neutrino Background ( $C\nu B$ ) is a long standing highly important scientific goal [95, 209, 240]. Analogous to the CMB, it carries a photographic image of the early Universe, albeit from a much older epoch of neutrino decoupling. Indirect evidence for the existence of the relic neutrinos was found in the observed  $C\nu B$  [82], however, due to the extreme weakness of the interactions between neutrinos and other forms of matter, direct detection of the  $C\nu B$  remains a major experimental challenge.

Today it is widely accepted that the most practicable route to the direct detection of the  $C\nu B$  lies through the measurement of the fine structure of the  $\beta$ -spectrum of a radioactive element [84–87, 95]. The main challenges are: the weakness of the signal which can be only compensated by the large amounts of the radioactive atoms (at least 100 g in order to achieve one event per year in the case of atomic Tritium) and the need in the extraordinary high energy resolution (50 meV or better) of the experiment.

So far, the only the only known way to overcome these roadblocks is a solid state architecture where the  $\beta$ -emitters are adsorbed on a substrate [96]. Such a design can increase the event count by orders of magnitude while preserving the necessary degree of control over the emitted electrons.

State-of-the-art PTOLEMY experiment [96] that exploits Tritium adsorbed

on the graphene motivated deeper theoretical studies of the physics of the  $\beta$ -decay in the vicinity of the solid state substrate [91, 241, 242]. It was revealed, that deposition of  $\beta$ -emitters on a solid-state substrate produces a new intrinsic fundamental limitation on the experimental resolution originating in the zero-point motion of the emitter's centre of mass [91]. This limitation strongly depends on the properties of the  $\beta$ -emitter such as its mass and energy released in  $\beta$  decay. While for Tritium it yields the uncertainty in the spectrum that is of the order  $\Delta E \sim 0.5$  eV, heavier emitters such as  $^{171}\text{Tm}$  and  $^{151}\text{Sm}$  reduce it by an order of magnitude [91, 242].

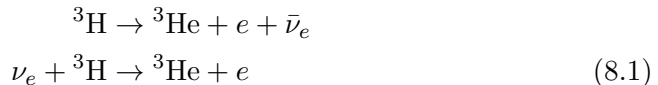
Zero point motion is not the only effect that leads to the intrinsic energy uncertainty [92, 241]. Solid state substrate hosts a whole zoo of elementary excitations which will affect the intrinsic uncertainty of the detector through a range of mechanisms. Each of those has to be studied one by one in order to find the ways to mitigate it.

This paper offers a second step into the physics of the  $\beta$ -decay of the emitter bounded to a solid state substrate. After the first and most simple mechanism of the emitter zero point motion was understood and the ways to mitigate it were found [91, 242], we proceed to, subjectively, second most simple and important effect - electromagnetic interaction of the  $\beta$ -decaying system and substrate. Specifically, we consider two kinds of processes: screening of the Helium ion by the charges in graphene and promotion of the graphene electrons from the valence to conduction band by the electric field of the emitted  $\beta$ -electron.

For simplicity, we assume that the decaying atom is Tritium, although the calculation can be straightforwardly generalized to the arbitrary atom.

## 8.2 Defining the problem

Consider mono-atomic Tritium deposited on graphene sheets arranged into a parallel stack where a clever magneto-electric design is used to extract and measure the energy of the electrons created in the two  $\beta$ -decay channels.



As a result of these processes, a Helium ion is formed and a  $\beta$ -electron is emitted. Both the ion and the emitted electron interact electromagnetically with each other and with the surroundings, namely graphene substrate. While the former is also present in the vacuum and its effect is accounted for in what

we call the “bare”  $\beta$ -decay spectrum [230], the effect of the latter two on the bare spectrum has to be evaluated. Let us try to do it treating each of them independently:

1. *Electromagnetic interaction of the Helium ion with the substrate.* Conversion of the tritium atom into Helium ion acts as a sudden creation of the charged impurity that brings the electrons in graphene out of equilibrium. The corresponding rearrangement of the charges  $Q(\vec{r}, t)$  (see Fig. 8.1) leads to a higher charge concentration near the impurity that would effectively screen it. This reduces the interaction strength between the emitted  $\beta$ -electron and Helium ion thus changing the  $\beta$ -spectrum.
2. *Electromagnetic interaction of the emitted  $\beta$ -electron with the substrate.* Before reaching the detector, emitted  $\beta$ -electron can scatter on the electrons in graphene promoting them from the valence to conduction band. Each of such processes is accompanied by the energy loss of the emitted electron equivalent to  $\Delta E = v_F(|p| + |p'|)$ , where  $\vec{p}, \vec{p}'$  are respectively the initial and final momenta of the electron in graphene thus also changing the  $\beta$ -spectrum.

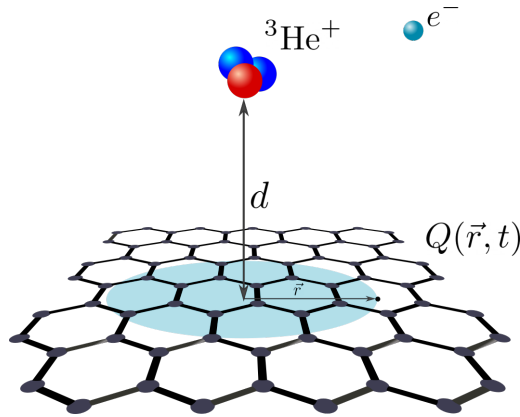


**Figure 8.1.** Schematic picture of screening mechanism in the graphene after the  $\beta$  decay of the Tritium bounded at the distance  $d$  from the substrate. As a result, a Helium ion is formed that leads to the rearrangement of the charges  $Q(\vec{r}, t)$  in the graphene. These charges screen the potential of the ion therefore performing work on the emitted  $\beta$ -electron.

Both of the processes described above have stochastic character (screened charge  $Q(\vec{r}, t)$  can have quantum fluctuations while the scattering of the elec-

tron on graphene is intrinsically probabilistic) which means that the change in the energy of the emitted  $\beta$ -electron is described by some distribution function  $\mathcal{F}(\cdot)$  and the initial  $\beta$ -spectrum  $\mathcal{G}(\cdot)$  changes to

$$\tilde{\mathcal{G}}(E_e) = \int d\varepsilon \mathcal{F}(\varepsilon) \mathcal{G}(E_e + \varepsilon) \quad (8.2)$$

if one is to account for the corresponding interaction process.

For simplicity, we discuss both the screening and electron scattering processes independent from all the other effects such as zero point motion, etc. [91] and independent from each other. So,  $\mathcal{G}(\cdot)$  is taken to be the one for the electron emitted by a free Tritium atom at rest.

### 8.3 Charge screening effects

Let us start from studying the effect of the screening of the Helium potential by electrons in graphene. In this case, the distribution function  $\mathcal{F}(\cdot)$  in Eq. (8.2) corresponds to the distribution of the work performed by the induced charge  $Q(\vec{r}, t)$  on the  $\beta$ -electron.

In this work, however, we are only going to calculate the average work  $\langle W(E_e) \rangle$  that is a purely classical contribution leaving out the calculation of the quantum fluctuations for the future studies. Large values of the average work ( $\langle W(E_e) \rangle \gtrsim m_\nu$ ) is going to be a signal that quantum mechanical fluctuations should be also taken into account. We also neglect the back-reaction of the induced charge on the ion assuming that it is fixed.

First, we make a dimensional estimate of the classical screening effect. The only dimension-full parameters relevant to this problem are:

1. Distance from the graphene substrate to the atom  $d \approx 3 \text{ \AA}$
2. Fermi velocity in graphene  $v_F \approx 10 \text{ \AA fs}^{-1}$ .

According to it, the typical time scale  $\tau_{\text{relax}}$  at which the electrons in graphene would screen the Helium ion can be estimated as

$$\tau_{\text{relax}} = \frac{d}{v_F} \approx 0.3 \times 10^{-15} \text{ s}. \quad (8.3)$$

During the relaxation time  $\tau_{\text{relax}}$ , the electron will fly away on the distance  $\lambda = v_\beta \tau_{\text{relax}}$ , where  $v_\beta$  is the typical velocity of the  $\beta$ -electron. For region of our interest that is the end of the  $\beta$  spectrum it that can be estimated as

$$\frac{v_\beta}{c} = \sqrt{\frac{2Q}{m_e c^2} \left( 1 + \underbrace{\frac{U}{Q}}_{\approx 0.001} \right)} \approx \frac{v_\infty}{c} \approx 0.27, \quad (8.4)$$

where  $Q = 18.6 \text{ keV}$  is the energy released in the  $\beta$ -decay and  $U$  is a Coulomb potential from the Helium ion that electron feels right after the decay.

This means that at the moment when the Helium ion is fully screened by the charges in the graphene,  $\beta$ -electron will fly away on

$$\lambda = v_\beta \tau_{\text{relax}} \approx 243 \text{ \AA}. \quad (8.5)$$

The difference in  $\beta$ -electron energy compared to unscreened case  $\Delta E_e$  is

$$\Delta E_e = k \frac{Z e^2}{\lambda} \approx 59 \text{ meV} \quad (8.6)$$

We see that already the classical effect of the charge screening in graphene leads to a significant shift in the  $\beta$ -electron energy  $\Delta E_e \gtrsim m_\nu$  that is comparable to the size of the energy gap that we want to measure.

The full quantum-mechanical calculation for the case of the perpendicular emission was also done using the linear response theory (see Appendix ??). The average work performed by the induced charge on the  $\beta$ -electron emitted with the velocity  $v_e$  is

$$\langle W(v_e) \rangle = \frac{\overbrace{\pi \alpha^2}^{\approx 0.5 \text{ eV}}}{16 E_F d^2} \tilde{W} \left( \frac{v_F}{v_e} \right), \quad (8.7)$$

where  $\tilde{W} \left( \frac{v_F}{v_e} \right)$  is defined by Eq. (8.21) and shown on (see Fig. 8.2).

For the  $\beta$ -electron at the edge of the spectrum ( $E_e = Q$ ), Eq. (8.7) yields  $\langle W(E_e = Q) \rangle \approx 75 \text{ meV}$ . This result is in a very good agreement (same order of magnitude) with the one that we have obtained with the simple estimate (8.6). We also see that the parameter that defines the relaxation time is indeed Fermi velocity in graphene  $v_F$ . The energy dependence of the work has the form of zeroth order Bessel function of the first kind  $\langle W(E_e) \rangle \sim J_0 \left( \sqrt{E_F/E_e} x \right)$  (see Fig. 8.2).

We emphasise, however, that despite the fact that the uncertainty in the energy of the  $\beta$ -electron at the edge of the spectrum is rather big as compared

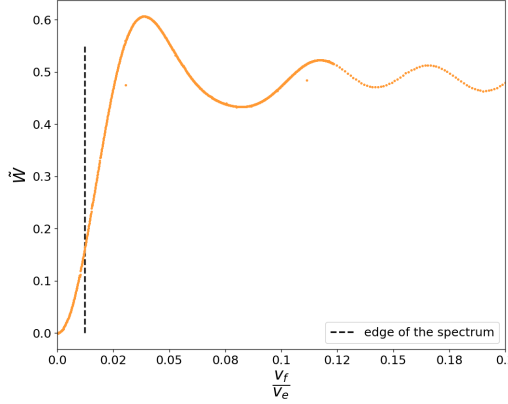


**Figure 8.2.** Average work (Eq. (8.21)) performed by the induced charges in graphene on the emitted  $\beta$ -electron depending on the ratio of the Fermi velocity in graphene  $v_F \approx 0.3 \times 10^{-15} \text{ s}$  to the velocity of the  $\beta$ -electron  $v_e$ .

to the required energy precision,  $\Delta E_e \approx 75 \text{ meV} \gtrsim m_\nu$ , it is not the right quantity that determines the final energy precision of the experiment. Instead, one should look at the functional dependence of the  $\langle W(E_e) \rangle$ , namely at the derivative like  $d\langle W(E_e) \rangle/dE_e$  since it determines the *relative* shift of the points of the spectrum. For example, if  $d\langle W(E_e) \rangle/dE_e \equiv 0$ , the whole spectrum will just shift and the energy gap between the bulk  $\beta$ -decay spectrum and neutrino capture part will remain unchanged.

$$|dW(E_e)| = \frac{\gamma}{2E_e} \frac{dW(\gamma)}{d\gamma} dE_e, \quad (8.8)$$

where we denoted  $\gamma = \sqrt{E_F/E_e}$ . For the edge of the spectrum,

$$|dW(E_e)|/dE_e|_{E_e=Q} \sim 10^{-5}.$$

This means that all the energies simply get “shifted” by the same amount and the gap in the spectrum does not disappear.

To conclude the analysis above, the classical screening effects in the graphene substrate appear to only lead to the total nearly constant energy shift of the end of the spectrum. This shift should be back-engineered and does not lead to any limitations on the energy resolution of the experiment.

Nevertheless, since the classical (mean) part of the work distributing appeared to be rather big, one needs to also study quantum charge fluctuations

$\sigma(W) = \langle \hat{W}^2 \rangle - W^2$ . As opposed to the classical effect, these lead to the irreducible changes in the spectrum. We leave the latter for future studies.

## 8.4 Electron-hole pair creation

The other electromagnetic effect that we consider in this work is the scattering process where the electron in graphene is promoted from the valence to the conduction band with possible momentum transfer  $\vec{p} \rightarrow \vec{p}'$ . As a result,  $\beta$  electron changes its momentum as well  $\vec{p}_\beta \rightarrow \vec{p}'_\beta$ .

Let us first estimate the average number such processes  $N_{\text{sc}}$  that will happen until the  $\beta$ -electron will leave the system. Using the Fermi Golden Rule (for the full calculation see Appendix ??), we obtain

$$N_{\text{sc}} = \frac{m_e}{v_\perp} \left( \frac{\kappa e^2}{2\pi} \right)^2 \int d^2q d^2p \frac{1 - \cos(\varphi(\vec{p}) - \varphi(\vec{q} + \vec{p}))}{p_\beta^\perp ((p_\beta^\perp - p_\beta'^\perp)^2 + q^2)^2} \quad (8.9)$$

where  $p_\beta^\perp = \sqrt{m_e v_F (|\vec{p}| + |\vec{q} + \vec{p}|) - (\vec{q} - \vec{p}_\beta^\parallel)^2 + p_\beta^2}$ .

For the  $\beta$ -decay of Tritium, the typical velocity of the emitted electron is  $v = 0.3c$ . We use system of units, where  $c = 1$ ,  $m_e = 1$  (and so  $\kappa e^2 = 14.4 \text{ eV \AA} = 7.5 \cdot 10^{-3}$  and  $v_F = 10 \text{ \AA fs}^{-1} = 3.3 \cdot 10^{-3}$ ). We see that  $v_e \gg v_F$ , so let us for simplicity re-scale everything introducing  $\vec{u} = \vec{q}/v_e$ ,  $\vec{w} = \vec{p}/v_e$  and write down an approximate simplified expression

$$N_{\text{sc}}^{3\text{H}}(\theta) = \frac{1.6 \times 10^{-5}}{\cos^2 \theta} \times I(\theta) \\ I(\theta) = \int d^2u d^2w \frac{1 - \cos(\varphi(\vec{w}) - \varphi(\vec{u} + \vec{w}))}{((\cos \theta - \delta(\theta, \vec{u}, \vec{w}))^2 + u^2)^2}, \quad (8.10)$$

where  $\theta$  is the emission angle with respect to the perpendicular to the graphene and  $\delta(\vec{u}, \vec{w}) = \sqrt{0.01(|\vec{w}| + |\vec{u} + \vec{w}|) - (\vec{u} - \sin \theta \vec{e}_\beta^\parallel)^2 + 1}$  ( $\vec{e}_\beta^\parallel$  is a projection of the initial  $\beta$ -electron velocity vector on the graphene plane).

It can be seen that the integral in Eq. (8.10) has both UV and IR divergences. However, one can introduce two natural cut-offs:

- IR cutoff that is defined by the system size ( $0.4 \cdot 10^{-12}$  for the system-size of 1 m).
- UV cutoff that is defined by the graphene lattice spacing ( $1/a = 1/(2.46 \text{ \AA}) = 1.5 \cdot 10^{-3}$ ).



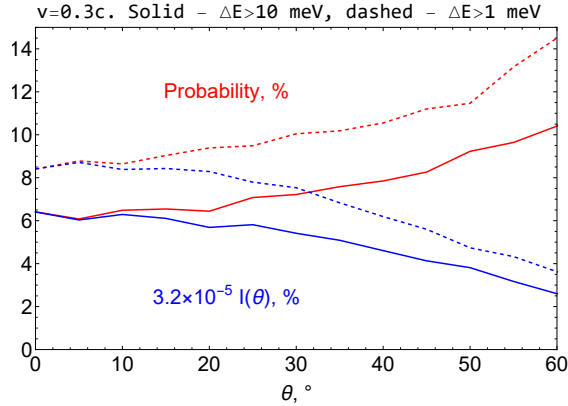


**Figure 8.3.** Red line: probability that the emitted electron will create a particle-hole excitation in graphene before it leaves the detector as a function of the emission angle  $\theta$ . The velocity of the emitted electron is  $0.3c$ . Blue line: value of the integral 8.10 for the same parameters. The solid and dashed lines correspond to different infra-red cut-offs that are defined by the size of the detector.

## 8.5 Conclusions

Solid state materials host a whole zoo of elementary excitations which will affect the intrinsic uncertainty of the detector through a range of mechanisms. For example, the sudden emission of an electron from a beta-decayer leaves behind a positively charged centre which attracts the electric current carriers in of the substrate. This effect results in what is known as the X-ray edge anomaly - a gamma-shaped broadening of the emission peak [92]. Other effects include the creation of vibrational excitations of the lattice, distortion of the spectrum due to the interaction of the beta-electron with its image charge, creation of shock wave emission due to the motion of the emitted electron at grazing angles at speeds exceeding the Fermi velocity, emission of plasmons and surface polaritons. The investigation of all these mechanisms and finding ways of mitigation requires a close collaboration between high-level experts in both theoretical and experimental solid state physics and may lead to further modifications of the experimental architecture.

## 8.6 Appendix: Average work performed by the electrons in graphene on the emitted $\beta$ -electron

Define  $Q(r, t)$  to be the total charge that has flown into the circle of radius  $r$  during the time  $t$  (See Fig. 8.1). For simplicity, we restrict ourselves to the case when the electron is emitted perpendicular to the substrate. Due to the rotational symmetry, it only depends on the absolute value of the distance  $r$ . Then, the total electrostatic potential at the point  $\vec{r}$  (see Fig. 8.1) is

$$\varphi_{\text{tot}}(r, t) = \varphi_{\text{bare}}(r) + k \frac{Q(r, t)}{r}, \quad (8.11)$$

where  $\varphi_{\text{bare}}(r) = -ke/\sqrt{r^2 + d^2}$  is the electrostatic potential of the bare Helium ion at the corresponding point. Performing the Fourier transformation gives:

$$\varphi_{\text{tot}}(q, \omega) = \varphi_{\text{bare}}(q) + 2\pi k \int_0^\infty dr J_0(qr) Q(r, \omega), \quad (8.12)$$

where  $J_n(x)$  is  $n^{\text{th}}$  Bessel function of the first kind.

The total electrostatic potential (8.12) can be also deduced from the response function of the graphene on charge impurity, so-called *polarization operator*  $\Pi(\omega, q)$  or, alternatively, its dielectric permittivity  $\varepsilon(\omega, q)$  [128]:

$$\varphi_{\text{tot}}(\omega, q) = \frac{1}{\varphi_{\text{bare}}^{-1}(q) - \Pi(\omega, q)} = \frac{\varphi_{\text{bare}}(q)}{\varepsilon(\omega, q)}. \quad (8.13)$$

The form of the polarization operator (or dielectric permittivity) depends on the type of the relaxation we are considering. We consider intrinsic (undoped) graphene where two valleys are independent, so no intra-valley scattering. In this case, the random phase approximation approach gives the following results for the polarization operator and dielectric permittivity [243]:

$$\Pi(q, t) = \frac{q^2}{8} J_0(v_F q t) \quad (8.14)$$

$$\varepsilon(q, t) = \left( \delta(t) + \frac{\alpha\pi}{4} q e^{-qd} J_0(v_F q t) \right), \quad (8.15)$$

where  $v_F$  is the Fermi velocity in graphene and  $\alpha = ke^2$ .

By requiring Eqns. (8.12),(8.13) be self-consistent, we can calculate the induced charge  $Q(r, t)$ :

$$\frac{\varphi_{\text{bare}}(q)}{2\pi k} \left( \frac{1}{\varepsilon(\omega, q)} - 1 \right) = \int_0^\infty dr J_0(qr) Q(r, \omega) \quad (8.16)$$

Using the orthogonality identity for Bessel functions  $\int_0^\infty x J_0(ux) J_0(vx) dx = \frac{1}{u} \delta(v - u)$  and the fact that  $\varphi_{\text{bare}}(q) = -e^{-qd} \times 2\pi k e/q$ , we find:

$$Q(r, \omega) = e \int_0^\infty r e^{-qd} J_0(qr) \left( 1 - \frac{1}{\varepsilon(\omega, q)} \right) dq. \quad (8.17)$$

The induced charge (8.17) creates repulsive Coulomb force  $F_{\text{ind}}$  acting on the  $\beta$ -electron that is flying away from the surface. Let us restrict ourselves to the case where the electron is flying away perpendicular from the surface. We believe that the result will be the same up to a pre-factor of order one for any emission angle due to the nature of the process. In this simplified case, due to the rotational symmetry, the force is perpendicular to the substrate and has the following magnitude:

$$F_{\text{ind}}(h) = ke(h + d) \int \frac{\partial_r Q(r, t) dr}{(r^2 + (h + d)^2)^{3/2}}, \quad (8.18)$$

where  $h = v_e t$  is the distance from the electron to the Helium ion. The corresponding work performed by the induced charge (8.17) on the  $\beta$ -electron is:

$$\langle W(E_e) \rangle = \int_0^\infty dh F_{\text{ind}}(h), \quad (8.19)$$

where we have neglected the deceleration of the electron. This is justified for the electrons near the edge of the spectrum <sup>1</sup>. Plugging in all the expressions, we obtain the final result

---

<sup>1</sup>The initial velocity  $v_0$  of the emitted electron is related to its velocity on infinity  $v_\infty$  as follows:

$$v_\infty = v_0 \sqrt{1 - \frac{2ke^2}{m_e d} \frac{1}{v_0^2}} = v_0 \sqrt{1 - \underbrace{\frac{0.18 \times 10^{-4} c^2}{v_0^2}}_\delta} \quad (8.20)$$

Since  $v_0 \approx 0.3c, \delta \ll 1$ , so  $v_\infty \approx v_0$ .

$$\begin{aligned}
 \langle W(v_e) \rangle &= \frac{\overbrace{\pi\alpha^2}^{\approx 0.5 \text{ eV}}}{16E_F d^2} \tilde{W}\left(\frac{v_F}{v_e}\right) \\
 \tilde{W}\left(\frac{v_F}{v_e}\right) &= \int_0^\infty y \left(1 - (1 + 2y)e^{-2y}\right) J_0\left(\frac{v_F}{v_e}y\right) dy \int_0^\infty \frac{(J_0(x) - xJ_1(x))}{(x^2 + y^2)^{3/2}} dx
 \end{aligned} \tag{8.21}$$

## 8.7 Appendix: Cross section of the process of the electron-hole creation in graphene

We denote  $d\omega_{i \rightarrow f}$  - the probability per unit time of the following event:  $\beta$ -electron with the momentum  $\vec{p}_\beta$  scatters with the electron in graphene that is in the valence band having momentum  $\vec{p}$ . After the scattering,  $\beta$ -electron changes its momentum to  $\vec{p}'_\beta$  and the electron in graphene is promoted to the conduction band with momentum  $\vec{p}'$ . According to the Fermi Golden Rule, it is equal to

$$\begin{aligned}
 d\omega_{i \rightarrow f}(\vec{p}_\beta, \vec{p}; \vec{p}'_\beta, \vec{p}') &= 4\pi \left| \int d^2\vec{\rho} d^2\vec{\rho}' dz' \langle \psi_f(\vec{p}'_\beta, \vec{p}') | \hat{W}(\vec{\rho}, \vec{\rho}', z') | \psi_i(\vec{p}_\beta, \vec{p}) \rangle \right|^2 \times \\
 &\times \delta\left(\frac{p'^2_\beta - p^2_\beta}{2m_e} - v_F(|p| + |p'|)\right) \frac{VS^2 d^3\vec{p}'_\beta d^2\vec{p} d^2\vec{p}'}{(2\pi)^7},
 \end{aligned} \tag{8.22}$$

where the additional factor 2 is accounted for that comes from the summation over the valleys in graphene. We assume that the initial  $\beta$ -electron has fixed chirality therefore it does not contribute to the sum. Writing down the interaction potential explicitly

$$\hat{W}(\vec{\rho}, \vec{\rho}', z') = \kappa e^2 \frac{\hat{\phi}^\dagger(\vec{\rho}', z') \hat{\phi}(\vec{\rho}, z') \hat{\psi}^\dagger(\vec{\rho}) \hat{\psi}(\vec{\rho})}{\sqrt{z'^2 + (\vec{\rho} - \vec{\rho}')^2}}, \tag{8.23}$$

where Fourier decomposition for field operators of the  $\beta$ -electron ( $\hat{\phi}$ ) and electron in graphene ( $\hat{\psi}$ ) are <sup>2</sup>

$$\hat{\phi}(\vec{\rho}, z) = \sum_s \int_{-\infty}^{\infty} \frac{d^3 \vec{k}}{(2\pi)^3} \frac{1}{\sqrt{2V E_{\vec{k}}}} e^{i(\vec{k}_{\parallel} \vec{\rho} + k_{\perp} z)} \left( \hat{c}_{\vec{k}}^s \tilde{u}^s(\vec{k}) + \hat{d}_{-\vec{k}}^s \tilde{v}^s(-\vec{k}) \right) \quad (8.24)$$

$$\hat{\psi}(\vec{\rho}) = \sum_{\alpha} \int_{-\infty}^{\infty} \frac{d^2 \vec{p}}{(2\pi)^2} \frac{1}{\sqrt{2S}} e^{i\vec{p}\vec{\rho}} \left( \hat{a}_{\vec{p}}^{\alpha} u^{\alpha}(\vec{p}) + \hat{b}_{-\vec{p}}^{\alpha} v^{\alpha}(-\vec{p}) \right). \quad (8.25)$$

The initial and final states are

$$|\psi_i\rangle = c_{p_{\beta}}^{\dagger} |FS\rangle, \quad |\psi_f\rangle = c_{p'_{\beta}}^{\dagger} a_{p'}^{\dagger} b_{-p} |FS\rangle. \quad (8.26)$$

Plugging everything in and treating  $\beta$ -electrons in the non-relativistic limit we arrive at

$$\begin{aligned} d\tilde{\omega}_{i \rightarrow f}(\vec{p}_{\beta}, \vec{p}; \vec{p}'_{\beta}, \vec{p}') &= \frac{\pi}{4V} (\kappa e^2)^2 \times \\ &\times \left| \int d^2 \vec{\rho} d^2 \vec{\rho}' dz' \frac{e^{i(\vec{p}_{\beta}^{\parallel} - \vec{p}'_{\beta}^{\parallel}) \vec{\rho}' + i(p_{\beta}^{\perp} - p'_{\beta}^{\perp}) z'}}{\sqrt{E_{\vec{p}_{\beta}} E_{\vec{p}'_{\beta}}} \sqrt{z'^2 + (\vec{\rho} - \vec{\rho}')^2}} e^{i(\vec{p} - \vec{p}') \vec{\rho}} \tilde{u}^{\dagger}(\vec{p}'_{\beta}) \tilde{u}(\vec{p}_{\beta}) u^{\dagger}(\vec{p}') v(-\vec{p})} \right|^2 \times \\ &\times \delta \left( \frac{p_{\beta}^{\prime 2} - p_{\beta}^2}{2m_e} - v_F (|\vec{p}| + |\vec{p}'|) \right) \frac{d^3 p'_{\beta} d^2 p' d^2 p}{(2\pi)^7}. \end{aligned} \quad (8.27)$$

The integral can be evaluated to be

$$\begin{aligned} d\tilde{\omega}_{i \rightarrow f}(\vec{p}_{\beta}, \vec{p}; \vec{p}'_{\beta}, \vec{p}') &= \frac{4\pi^3 S}{V} (\kappa e^2)^2 \frac{\left| \tilde{u}^{\dagger}(\vec{p}'_{\beta}) \tilde{u}(\vec{p}_{\beta}) u^{\dagger}(\vec{p}'_{\beta}^{\parallel} + \vec{p} - \vec{p}'_{\beta}^{\parallel}) v(-\vec{p}) \right|^2}{((p_{\beta}^{\perp} - p'_{\beta}^{\perp})^2 + (p_{\beta}^{\parallel} - p'_{\beta}^{\parallel})^2)^2 E'_{\beta} E_{\beta}} \times \\ &\times \delta \left( \frac{p_{\beta}^{\prime 2} - p_{\beta}^2}{2m_e} - v_F (|\vec{p}| + |\vec{p}_{\beta}^{\parallel} + \vec{p} - \vec{p}'_{\beta}^{\parallel}|) \right) \frac{d^3 p'_{\beta} d^2 p}{(2\pi)^5}. \end{aligned} \quad (8.28)$$

The spinors of the  $\beta$ -electron are

$$\tilde{u}(\vec{p}_{\beta}) = \sqrt{2E_{\vec{p}_{\beta}}} \vec{\chi}, \quad \text{where } \vec{\chi}_+ = (0, 0, 1, 0), \vec{\chi}_- = (1, 0, 0, 0), \quad (8.29)$$

---

<sup>2</sup>We note that we distinguish electrons in graphene and  $\beta$ -electron. Namely, no exchange can occur.

where  $\bar{\chi}$  denotes chirality. The spinors of the electron in graphene are

$$u^\alpha(p) = \frac{1}{\sqrt{2}} \begin{pmatrix} 1 \\ \alpha e^{i\varphi(p)} \end{pmatrix}, \quad v^\alpha(-p') = \frac{1}{\sqrt{2}} \begin{pmatrix} 1 \\ -\alpha e^{i\varphi(p')} \end{pmatrix} \quad (8.30)$$

with  $\varphi(p) = \arctan(p_y/p_x)$ . So, we arrive at

$$\begin{aligned} d\tilde{\omega}_{i \rightarrow f}(\vec{p}_\beta, \vec{p}; \vec{p}'_\beta, \vec{p}') &= \frac{(2\pi)^3 S}{V} (\kappa e^2)^2 \frac{1 - \cos(\varphi(\vec{p}) - \varphi(\vec{p}'_\beta + \vec{p} - \vec{p}'_\beta))}{((p_\beta^\perp - p'^\perp_\beta)^2 + (p_\beta^\parallel - p'^\parallel_\beta)^2)^2} \times \\ &\times \delta\left(\frac{p'^2_\beta - p^2_\beta}{2m_e} - v_F(|p| + |p'_\beta + \vec{p} - p'_\beta|)\right) \frac{d^3 p'_\beta d^2 p}{(2\pi)^5}. \end{aligned} \quad (8.31)$$

where  $\varphi(\vec{k})$  denotes the angle in the polar coordinate system of the vector  $\vec{k}$ . The total probability per unit time of the transition into any final state can be obtained by integrating over all final states

$$\frac{dP}{dt} = \frac{(2\pi)^2 S m_e}{V} (\kappa e^2)^2 \int \frac{d^2 q d^2 p}{(2\pi)^4} \frac{1 - \cos(\varphi(\vec{p}) - \varphi(\vec{q} + \vec{p}))}{p'^\perp_\beta ((p_\beta^\perp - p'^\perp_\beta)^2 + q^2)^2}, \quad (8.32)$$

where  $\vec{q} = \vec{p}'_\beta - \vec{p}'_\beta$  and  $p'^\perp_\beta(\vec{q}, \vec{p}) = \sqrt{m_e v_F(|\vec{p}| + |\vec{q} + \vec{p}|) - (\vec{q} - \vec{p}'_\beta)^2 + p^2_\beta}$  due to energy conservation. In other words, the inverse time of a single interaction  $\tau$  is

$$\frac{1}{\tau} = \frac{(2\pi)^2 S m_e}{V} (\kappa e^2)^2 \int \frac{d^2 q d^2 p}{(2\pi)^4} \frac{1 - \cos(\varphi(\vec{p}) - \varphi(\vec{q} + \vec{p}))}{p'^\perp_\beta ((p_\beta^\perp - p'^\perp_\beta)^2 + q^2)^2}. \quad (8.33)$$

If the typical time that electron spends in the setup is  $t_{\text{measure}} = L/v_\perp = V/(Sv_\perp)$ , where  $v_\perp$  is the perpendicular component of the electron velocity then during this time electron will experience  $N_{\text{sc}} = t_{\text{measure}}/\tau$  number of events

$$N_{\text{sc}} = \frac{m_e}{v_\perp} \left(\frac{\kappa e^2}{2\pi}\right)^2 \int d^2 q d^2 p \frac{1 - \cos(\varphi(\vec{p}) - \varphi(\vec{q} + \vec{p}))}{p'^\perp_\beta ((p_\beta^\perp - p'^\perp_\beta)^2 + q^2)^2} \quad (8.34)$$

where  $p'^\perp_\beta(\vec{q}, \vec{p}) = \sqrt{m_e v_F(|\vec{p}| + |\vec{q} + \vec{p}|) - (\vec{q} - \vec{p}'_\beta)^2 + p^2_\beta}$ .

